Implementation and comparison of advanced behaviour laws for sheet metal forming

Sever-Gabriel Racz, Xavier Lemoine, Badis Haddag, Farid Abed-Meraim

Implementation and comparison of advanced behaviour laws for sheet metal forming

G. Racz[1*], X. Lemoine[1], B. Haddag[2], F. Abed-Meraim[2]

[1] *Arcelor Research S.A., Automotive Product, Customers Service, voie romaine BP 30320, F-57283 Maizière-lès-Metz, France*
e-mail: xavier.lemoine@arcelor.com;

[2]*Laboratoire de Physique et Mécanique des Matériaux, ENSAM Metz, 4 rue A. Fresnel, 57078 Metz Cedex 03, France*
e-mail: baddis.haddag@metz.ensam.fr, farid.abed-meraim@metz.ensam.fr

ABSTRACT: This contribution concerns the implementation in the FE code Abaqus/Explicit of anisotropic elastoplastic behaviour laws for sheet metal forming. Several hardening laws are considered: isotropic hardening (Swift, Voce), kinematical hardening (Armstrong-Frederick), combinations of both as well as the microstructural model of Teodosiu-Hu. The initial anisotropy is described by the Hill'48 yield function. A specific, explicit time integration scheme is developed for use with shell elements. The validation of the implementation and the comparison between the different hardening laws is made using rheological tests. Several, different monotonic tests are used: tensile test, shear test and plane strain test, together with two-path tests: tensile+shear and shear-to-shear (Bauschinger). A cross-shape cup drawing test is used as an application for a deeper comparison of the real benefit of the different hardening laws.

Key words: strain-path induced hardening, shell finite element implementation, explicit time integration

1 INTRODUCTION

Nowadays, considerable numerical techniques are more and more used, by the mechanical components manufacturers, for the analysis of forming processes. Formerly, expensive experimental studies were required to control and optimise these processes. Now, several researches and developments are carried out to bring new knowledge and new numerical tools to fill up the increasing industrial needs. The manufacturing of mechanical components with simulations allow, on one hand, a better understandings of the phenomena taking place during the forming process and on other hand, a better control of the quality of the product. The quality of the product is of course its geometry but also its material state: the metallurgical and mechanical properties of the final product. This point is essential for the prediction of a mechanical component during its later use. The current work concerns the numerical simulation of the deep drawing process, with emphasis on the coupling of enhanced constitutive models with commercially available FE codes. The following objectives have been drawn for this work:

- Development of a time integration algorithm for constitutive models and its implementation into commercially available dynamic explicit simulation codes as Abaqus/Explicit, for shell element.
- Validation of the implementation using rheological tests (monotonic or sequenced) as well as several drawing configurations, like the cross-shape cup drawing.

2 NUMERICAL IMPLEMENTATION

2.1 Equations of elastoplastic behaviour

A material description based on rate equations must respect the principle of objectivity. In finite element implementations, the most commonly used technique is to integrate the rate equations in a frame that rotates with the spin $\boldsymbol{W}$ (skew-symmetric part of the velocity gradient). This is equivalent to the use

[*] Corresponding author. On leave from the "Lucian Blaga" University from Sibiu, Romania.

of a Jaumann-type stress rate, yet the equations obtained are form- identical to a small strain formulation [1]. Consequently, all the tensor variables below are rotation-compensated with respect to this frame.
We consider elastic-plastic, anisotropic materials, defined by the following equations:
Yield function:

$$F(\boldsymbol{\sigma},\boldsymbol{X},R) := \sigma^{eq}(\boldsymbol{\sigma}'-\boldsymbol{X}) - Y_0 - R \qquad (1)$$

where $\boldsymbol{\sigma}$ is the stress tensor, $\boldsymbol{\sigma}'$ is its deviator, $\boldsymbol{X}$ and R are the internal variables describing the current position ($\boldsymbol{X}$; back-stress) and size increase (R) of the yield surface. The material becomes plastic when the yield function vanishes. Y_0 is the initial size of the yield surface.
Flow rule: we consider associated plasticity:

$$\boldsymbol{D}^p = \dot{\lambda}\boldsymbol{V} \quad ; \quad \boldsymbol{V} = \partial F / \partial \boldsymbol{\sigma} \qquad (2)$$

where $\boldsymbol{D}^p$ is the plastic strain rate, $\boldsymbol{V}$ is the gradient of the yield function and $\dot{\lambda}$ the plastic multiplier.
Hardening is governed by rate equation having the generic form below:

$$\dot{R} = \rho\dot{\lambda} \quad ; \quad \dot{\mathbf{X}} = \xi\dot{\lambda}, \qquad (3)$$

with the initial conditions $R(0) = 0$ and $\boldsymbol{X}(0) = \mathbf{0}$.
Hypo-elastic law:

$$\dot{\boldsymbol{\sigma}} = \boldsymbol{C} : (\boldsymbol{D} - \boldsymbol{D}^p), \qquad (4)$$

where $\boldsymbol{C}$ is the fourth order tensor of elastic constants and $\boldsymbol{D}$ is the total strain rate.
Tangent modulus: The plastic multiplier is computed using the consistency condition $\partial F/\partial t = 0$. After differentiation of eq. (1) and use of equations (2-4), one can write the plastic multiplier as:

$$\dot{\lambda} = \frac{\boldsymbol{V} : \boldsymbol{C} : \boldsymbol{D}}{\boldsymbol{V} : \boldsymbol{C} : \boldsymbol{V} + \boldsymbol{V} : \xi + \rho} \qquad (5)$$

This expression can be used whatever the particular yield surface and the hardening laws considered. If the tensor $\boldsymbol{C}$ is isotropic, this expression is further simplified:

$$\dot{\lambda} = \frac{2\mu \boldsymbol{V} : \boldsymbol{D}}{2\mu|\boldsymbol{V}|^2 + \boldsymbol{V} : \boldsymbol{\xi} + \rho}, \qquad (6)$$

where λ and μ are the elastic constants of Lamé.
Then, the elasto-plastic tangent modulus $\boldsymbol{L}$ can be derived:

$$L = \mathbf{C} - \alpha \frac{4\mu^2}{2\mu|\mathbf{V}|^2 + \mathbf{V} : \xi + \rho} \mathbf{V} \otimes \mathbf{V}, \qquad (7)$$

where α equals 1 for a plastic state and 0 otherwise.
So far, the material model has been developed in a general analytical framework. The yield function is defined by the equivalent stress σ^{eq} and its derivatives $\boldsymbol{V}$, while the hardening is defined by ρ and ξ. Most of the available material models fall into this framework:

- Yield criterion: Hill (1948), Von Mises
- Isotropic hardening laws: Swift, Voce
- Isotropic and kinematics hardening laws: cited isotropic laws (Voce or Swift) combined with saturating kinematical hardening law (Armstrong-Frederick [2])
- Physically-based hardening model: Teodosiu-Hu law [3].

2.2 Implementation of material model for solid elements

The computer implementation is based on the explicit time integration algorithm developed in [4]. The integration scheme consists of the following steps:
0) Input: $\Delta\boldsymbol{\varepsilon}$, state at time "$t$" (known)
1) Compute $F_t = \sigma^{eq}(\boldsymbol{\sigma}'_t - \boldsymbol{X}_t) - Y_0 - R_t$
2) If $(F_t) < 0$, elastic increment
3) Else, elastic-plastic increment:
Compute ρ, ξ, $\boldsymbol{L}$, $\Delta\lambda = \dot{\lambda}_t \Delta t$
Compute $\Delta R = \rho_t \Delta\lambda$, $\Delta\boldsymbol{X}$, $\Delta\boldsymbol{\sigma}$ etc.
4) Update state and return.
The advantage of this algorithm is that it remains very general; the yield locus and the hardening model can be integrated into this framework, without altering the overall structure.

2.3 Extension of the algorithm to shell elements

Shell elements are the most commonly used for the simulation of sheet metal forming, due to the aspect ratio of the sheet. From a computational viewpoint, this is more difficult than using solid elements, since now the plane stress condition has to be included. The generality of the overall algorithm should be preserved. This is accomplished by the use of the tangent modulus for computing the through-thickness (33) component of the strain increment. Then, the former (solid element) scheme is applied as before. Since the time integration scheme is

purely explicit, the use of the tangent modulus for enforcing the plane stress condition is consistent. In the following algorithm, the modifications corresponding to the shell element with respect to the solid element algorithm are shown in bold characters:

0) Input: $\Delta\boldsymbol{\varepsilon}$, state at time "$t$" (known)

A) Compute $\Delta\varepsilon_{33} = C_{33ij}\,\Delta\varepsilon_{ij} / C_{33ij}$

1) Compute $F_t = \sigma^{eq}(\boldsymbol{\sigma}'_t - \boldsymbol{X}_t) - Y_0 - R_t$

2) If $(F_t) < 0$, elastic increment

3) Else, elastic-plastic increment:

Compute L, $\Delta\varepsilon_{33} = L_{33ij}\,\Delta\varepsilon_{ij} / L_{33ij}$

Compute ρ, ξ, $\Delta\lambda = \dot{\lambda}_t \Delta t$

Compute $\Delta R = \rho_t \Delta\lambda$, $\Delta\boldsymbol{X}$, $\Delta\boldsymbol{\sigma}$ etc.

4) Update state and return.

Again, this algorithm can be adapted to any material model without any change.

3 VALIDATION ON RHEOLOGICAL PATHS

Several rheological tests, for Dual-phase steels, have been simulated with Abaqus/Explicit, using the vumat routines corresponding to the five hardening laws and two yield criteria. The rheological tests include monotonic tests and two-path tests: uniaxial tensile (TU), plane tensile (TP), biaxial (BS) and/or shear tests (SH). Some relevant results are given in the following picture, for Hill (1948) criterion and physically-based hardening model (Teodosiu-Hu law):

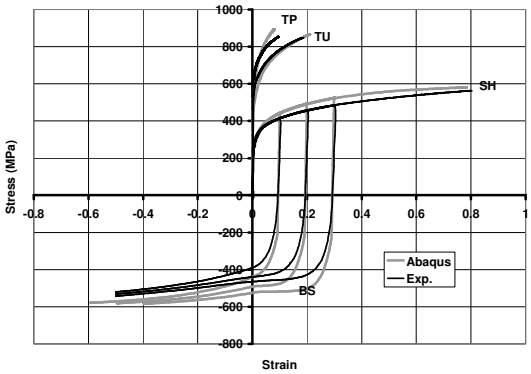

Fig. 1. Prediction of rheological paths

These results clearly validate the developed constitutive algorithm and its implementation in Abaqus. Thus, more involved applications have been simulated hereafter using this implementation.

4 APPLICATION: CROSS-SHAPE CUP TEST

4.1 Process conditions

The deep drawing simulations have been also performed in Abaqus/Explicit, using the vumat routine and shell elements (S4R). Vumat routines have been written for each hardening law / yield function. A versatile and modular software structure allows for easy change of the material law. A cross-shape cup drawing process has been investigated, both numerically and experimentally. From an experimental viewpoint, the draw-in has been measured together with a more involved in-plane strain measurement using the Asame system. Also, the experimental punch force has been recorded. The table summarize the principal process conditions.

Table1. Process conditions for cross-shape cup drawing

Blank-Holder Force	314 kN
Quaker 6130 oil - friction coefficient (μ)	0.1
Numerical punch speed: (experimental : 112 mm/s)	1 m/s
blank size:	280 x 280 mm
punch stroke:	25 mm

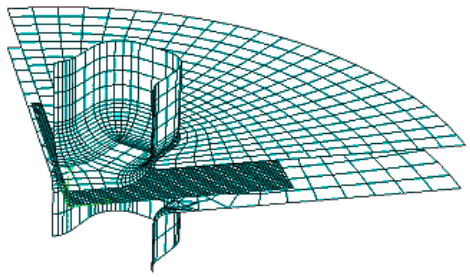

Fig. 2. FE model of cross-shape test (1/4 of the real geometry)

4.2 Results

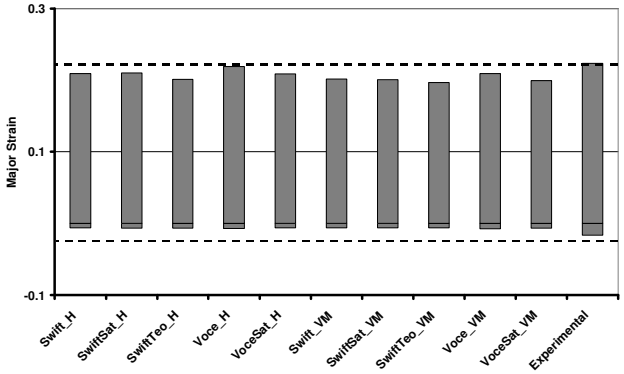

Fig. 3. Major strain interval on measure area (1/4 of part).

From the analysis of the minimum and maximum strain distributions one can conclude the following:

- The simulations predict strain distributions very similar to the experimental ones;

- Also, the strain values are very close;
- The predictions using the Hill'48 criterion are more accurate than the Mises ones;
- When the Hill'48 criterion is used, the most accurate hardening model appears to be the microstructural (Teodosiu-Hu) one;
- It is important to note that the differences between the different strain predictions (about 1%) are in the error range of the experimental measure with the Asame system (about 2%). Thus, more discriminating experiments or more accurate experimental measures should be used to further compare the behaviour laws.

The analysis of the predicted stresses reveals that:

- All the models predict very similar distributions of stress;
- Nevertheless, the maximum stress values in the part are very different from a model to another; thus, stress measurements might be a possibility to discriminate the models;
- Since the stresses cannot be measured at the end of the drawing, one possibility would be to simulate the stress unloading (springback) and to measure the residual stresses by means of X-Ray diffraction.

Concerning the draw-in, we find again the same result with classical numerical prediction. It seems the hardening laws have almost no influence on this measure, while the yield criterion does.

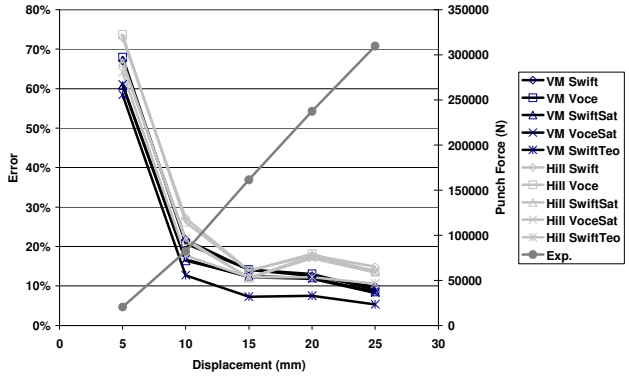

Fig. 4. Error [%] between experimental and predicted punch force

The predicted and experimental punch forces have the same time evolution and very close values. It seems that von Mises criterion gives best prediction than Hill (1948) criterion. For the hardening laws, the Teodosiu-Hu law provides the best prediction.

5 CONCLUSIONS

An algorithm for constitutive laws implementation in FEA codes, designed for solid elements [4] has been extended to shell finite elements and implemented in the dynamic explicit finite element code Abaqus/Explicit. This implementation has been validated on rheological tests (simple and two-path). A drawing test has been considered as final application. Experimental strain measurements have been performed on real drawn part using the Asame measurement system, together with the draw-in and the punch force.

The simulations are well validated by the experiments. Nevertheless, more accurate measurements are needed to better discriminate the different models. One solution could be the simulation of springback and the measurement of the residual stresses (by X-Ray diffraction), since the differences in the predicted stresses are higher than the differences in the predicted strains.

ACKNOWLEDGEMENTS

The authors are grateful to the European Commission who financially supported this work, through the Marie Curie Host fellowships. The authors thank the LPMTM of University Paris 13 for their experimental tests.

REFERENCES

1. A. Haddad, T. Balan, F. Abed-Meraim, On the implementation of hardening models in sheet forming simulations, Proc. 6th Int. Esaform Conf., Salerno, Italy, April 28-30 2003, pp. 187-190 (2003).
2. P.J. Armstrong, C.O. Frederick, A mathematical representation of the multiaxial Bauschinger effect, *Technical Report RD/B/N731,* CEGB (1966).
3. S. Bouvier, C. Teodosiu, H. Haddadi, V. Tabacaru, Anisotropic work-hardening behaviour of structural steels and aluminium alloys at large strains, *Proc. EMMC6-MECAMAT*, Liège (2002) 329-336.
4. B. Haddag, T. Balan, F. Abed-Meraim, Finite element prediction of strain-path induced anisotropy in deep drawing, Esaform Conf., Trondheim, avril 2004, pp. 491-494 (2004).